

Electron emission from disordered tetrahedral carbon

B. L. Weiss, A. Badzian, L. Pilione, T. Badzian, and W. Drawl

Citation: *Applied Physics Letters* **71**, 794 (1997); doi: 10.1063/1.119648

View online: <http://dx.doi.org/10.1063/1.119648>

View Table of Contents: <http://scitation.aip.org/content/aip/journal/apl/71/6?ver=pdfcov>

Published by the [AIP Publishing](#)

Articles you may be interested in

[Electron field emission properties of carbon nanotubes converted from nanodiamonds](#)

J. Vac. Sci. Technol. B **21**, 1688 (2003); 10.1116/1.1593643

[Electron field emission from boron-nitride nanofilms](#)

Appl. Phys. Lett. **80**, 3602 (2002); 10.1063/1.1477622

[Field emission from short and stubby vertically aligned carbon nanotubes](#)

Appl. Phys. Lett. **79**, 2079 (2001); 10.1063/1.1406557

[Electron field emission from Ti-containing tetrahedral amorphous carbon films deposited by filtered cathodic vacuum arc](#)

J. Appl. Phys. **88**, 6842 (2000); 10.1063/1.1323541

[Electron field emission from amorphous carbon nitride synthesized by electron cyclotron resonance plasma](#)

J. Vac. Sci. Technol. B **18**, 1840 (2000); 10.1116/1.1303813



Electron emission from disordered tetrahedral carbon

B. L. Weiss,^{a)} A. Badzian, L. Pilione,^{b)} T. Badzian, and W. Drawl

Materials Research Laboratory, The Pennsylvania State University, University Park, Pennsylvania 16802

(Received 1 April 1997; accepted for publication 10 June 1997)

Electron field-emission tests have been performed on films grown by a modified microwave plasma assisted chemical vapor deposition diamond process. This modification includes the addition of N₂ and O₂ during the growth stage. Characterization of these films shows the presence of a disordered tetrahedral carbon structure. Raman spectroscopy indicates a disturbance in the cubic symmetry of the lattice and x-ray diffraction indicates a disordered tetrahedral structure. Field-emission testing indicate that current densities of 0.5 mA/cm² can be obtained for applied fields of 5–8 V/μm. The results are explained in terms of a change in the band structure and the formation of electronic states in the band gap. © 1997 American Institute of Physics. [S0003-6951(97)00632-3]

Field emission of electrons by tunneling through the surface barrier at a metal–vacuum interface, due to an applied electric field, has been reported on extensively for sharp metal tips (Spindt cathodes).¹ These Spindt cathodes have shown promise for use in cold cathode devices. This is, in part, due to the curved geometry of the emitters, which enhance the emission characteristics.²

Thin-film devices have also shown promise for cold cathode applications. The treatment of internal field emission³ (IFE) led to the development of electron emission devices based on a metal–insulator–metal (MIM) device using thin (<0.1 μm) insulating films.⁴ The MIM devices have been used as a spectroscopic tool to study electron energy distributions of the vacuum emitted electrons.^{5,6} These studies have shown that the electrons can gain energy above the conduction-band minimum, and are termed hot electrons; the studies have also been used to gain insight into the dielectric breakdown behavior of the films.⁷ A considerable amount of the research has been done on SiO₂ thin films because of the materials' importance to the electronics industry.

Further development of these devices has led to the use of metal island injectors at the metal–insulator interface to enhance the IFE process.⁸ This is referred to as tunnel injection and is analogous to the Spindt emitters. Also, electron emission^{9–11} and Monte Carlo simulation^{7,12,13} studies have been carried out on metal–insulator–semiconductor–metal device thin films (≈0.01–0.1 μm). Monte Carlo simulations have recently been performed for thicker (≈1 μm) semiconducting films to study the ballistic nature of electron transport in the conduction band.¹⁴

A new stimulus for electron emission study came about when it was reported that diamond exhibited negative electron affinity^{15–17} (NEA) and that practical devices could be fabricated.^{18,19} Along with the NEA, it has also been demonstrated that diamond exhibits ballisticlike transport in the conduction band.¹⁴ Recently, Okano reported on a device fabricated from doped cubic diamond, with high nitrogen levels (10²⁰/cm³), by hot filament chemical vapor deposition

(CVD).²⁰ Nonperfect CVD diamond has also shown advantages in several electron emission studies.^{21,22}

In this letter, we report on electron emission from a thin-film structure based on a disordered tetrahedral carbon (DTC) prepared by a microwave plasma assisted chemical vapor deposition (MPACVD) diamond growth process, which is modified by the addition of N₂ and O₂ to the plasma. The results of the DTC films are compared to the results we have obtained from polycrystalline CVD diamond films.

The CVD diamond growth process enables the formation of tetrahedral forms of carbon, which differ from cubic diamond. We have proposed structural models based on the tetrahedral coordination of the carbon atoms for several polytypic forms.^{23,24} The models consider hexagonal stacking, nanoscale microtwinning, and displacement disorder of the carbon atoms. The addition of N₂ or O₂ results in different forms of tetrahedral carbon.^{23–25} This current study exploits a particular composition of CH₄, H₂, N₂, and O₂ in the plasma.

We have deposited DTC films on Mo substrates using a microwave plasma. The MPACVD system used for depositing the films consists of a 2.45 GHz tunable microwave cavity and a 1.5 in. diam silica tube.

The Mo substrate is polished with 600 grit SiC sandpaper and cleaned in an ultrasonic cleaner. The substrate is then seeded with <1 μm diamond powder and cleaned in a hydrogen plasma for 5–10 min. This process also heats the Mo to the desired deposition temperature of 875–925 °C, as measured by an optical pyrometer. The nucleation step consists of a 30–45 min 6% CH₄ (100% H₂ at 40 sccm and 10% CH₄/H₂ at 60 sccm) concentration. N₂ (10 sccm) and O₂ (0.3 sccm) are introduced into the plasma during the growth stage. The growth rate of the films is ≈0.3 μm/h.

Characterization of the films was carried out by Raman spectroscopy, x-ray diffraction (XRD), optical and scanning electron microscopy, and x-ray photoelectron spectroscopy. The Raman spectra (see Fig. 1) shows three broad peaks at 1190, 1340, and 1550 cm⁻¹. The 1550 cm⁻¹ peak has a full width at half-maximum of ≈30 cm⁻¹. This peak also appeared for DTC grown from a CH₄/N₂ mixture.²⁴ The lack of the 1332 cm⁻¹ peak indicates a disturbance of the cubic symmetry of the lattice.

^{a)}Electronic mail: blw8@email.psu.edu

^{b)}Present address: Department of Physics, The Pennsylvania State University, Altoona, PA 16601.

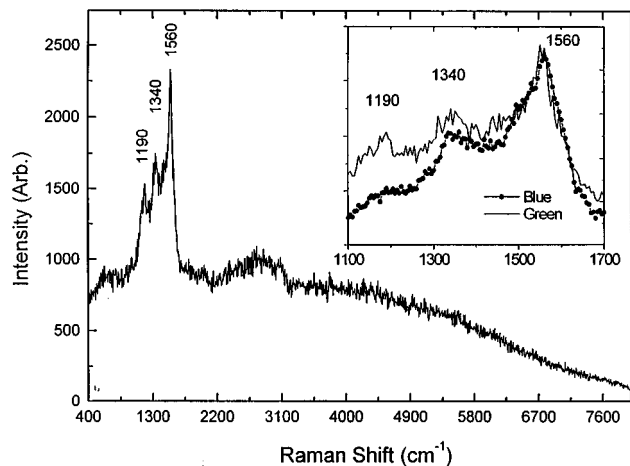


FIG. 1. Raman spectra for the disordered tetrahedral carbon films. The wavelength of the laser used is 514.5 nm. The inset contains a comparison of Raman spectra for 514.5 nm (green) and 488 nm (blue) lasers.

X-ray diffraction was recorded by the Debye–Scherrer method for Cu $K\alpha$ radiation. Two components of diffraction appeared on the pattern: scattering around the central beam and a set of weak broad peaks corresponding to the cubic diamond lines 111, 220, 331, and 331. The 220 line was shifted towards larger θ . No graphitic phase scattering was seen.

Combining the Raman and XRD data, we believe the atomic structure of the CVD films grown with N_2 and O_2 additions is highly disordered. The atomic network has tetrahedral coordination, but the local symmetry departs from that of cubic diamond. However, some type of long-range order still appears to exist within the crystal grains. Scanning electron microscopy of the films showed a columnar structure along the growth direction and a surface roughness of $<0.5 \mu\text{m}$.

Field-emission (FE) testing has been carried out on samples of different composition and thickness. A schematic of the test chamber is shown in Fig. 2. The FE test stage consists of a metal base for making electrical contact to the Mo substrate and an anode fastened to a micropositioner for varying the anode cathode spacing. The anode was a Duralloy™ probe from IDI with an area of $A=0.33 \text{ cm}^2$. The electrometer is a Keithley 6517 and the voltage supply is a Fluke 410B. The FE test stage is placed in a high vacuum chamber with a base pressure of 2×10^{-7} Torr, which can be reduced to 2×10^{-8} Torr by use of a liquid-nitrogen (LN2) trap.

FE testing was carried out on four types of films: $1 \mu\text{m}$ (thin) and $6 \mu\text{m}$ (thick) DTC and similar thickness polycrystalline CVD diamond films. The thin DTC films had a resistance of $\approx \text{k}\Omega$ and the thick films had resistances of $\approx \text{M}\Omega$. The CVD diamond films had resistances larger than $20 \text{ M}\Omega$. For the thin DTC films, calculated fields of $5\text{--}8 \text{ V}/\mu\text{m}$ (calculated field=applied voltage/film–anode spacing) have shown current densities of $0.5 \text{ mA}/\text{cm}^2$. The thicker DTC films did show an advantage over both the thick and thin diamond films. Calculated fields of $50\text{--}100 \text{ V}/\mu\text{m}$ yielded current densities of $3\text{--}5 \text{ mA}/\text{cm}^2$ for the thick DTC films and $\approx 1 \text{ mA}/\text{cm}^2$ for both CVD diamond films. The

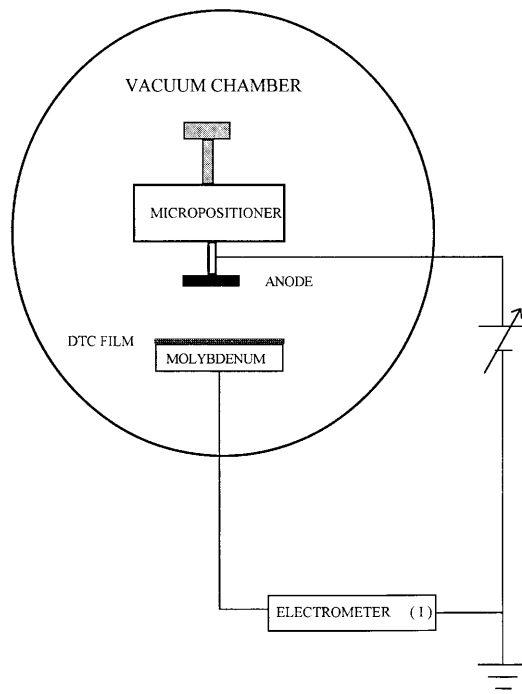


FIG. 2. Schematic of the field-emission testing chamber.

I – V and Fowler–Nordheim (FN) plots for the films are shown in Figs. 3 and 4, respectively.

The current–voltage characteristics also provide some insight into the breakdown nature of the films. Study of the emission characteristics of the films at fields higher than those stated above were not carried out due to electric breakdown. In the high-field regions (i.e., just before breakdown), localized emission sites may produce a short-lived high current burst. These current bursts are a precursor to the breakdown and, in our experiments, these bursts are quite noticeable and ultimately result in physical damage to the film.

Although the I – V characteristics plotted in FN coordinates yield an approximate straight line, we must caution that the field used here, applied voltage/film–anode spacing, is not necessarily the true local (or vacuum) field, which determines the shape of the barrier for the tunneling process.

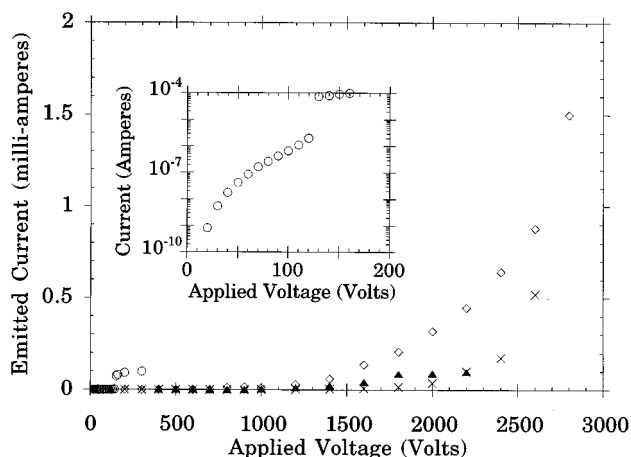


FIG. 3. I – V characteristics of the thin DTC films (○), the thick DTC film (◇), and the thin CVD (▲) and thick (×) CVD diamond films. Inset shows details of the $1 \mu\text{m}$ DTC film.

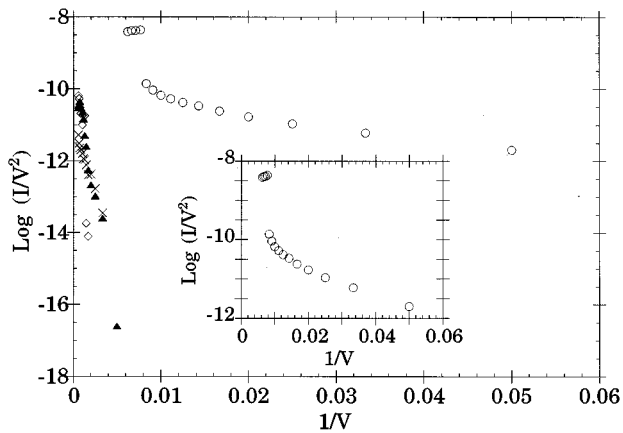


FIG. 4. FN plot for the thin DTC film (\circ), the thick DTC film (\diamond), and the thin CVD (\blacktriangle) and thick (\times) CVD diamond films. Inset shows details of the $1\ \mu\text{m}$ DTC film.

Rather, the doping level, electronic structure, or the insulating character of the film determines the potential distribution. This, in combination with other factors (e.g., transport through the film, etc.), determines the form of the potential profile at the interface and, thus, the current emission into the vacuum.²⁶

The results show an improvement in field-emission characteristics when the DTC films are compared to CVD diamond. The reason for the improvement in the emission characteristics is a subject of speculation. However, a change is evident in the atomic structure from cubic diamond to a disordered tetrahedral carbon. This involves a new configuration of tetrahedra, the introduction of N, O, and H atoms and nondiamond vibrational signatures as detected by Raman spectroscopy. When the atomic lattice of a single crystal loses its periodicity, the electronic structure of the material changes. Specifically, the formation of tails on the density of states at the valence-band maximum and conduction-band minimum and the introduction of additional electronic states in the band gap can be present.

DTC grown by a CVD diamond process with the addition of N_2 and O_2 show promise as a suitable material for cold cathode applications. The rearrangement of the electronic structure and an IFE mechanism suggests a physical explanation for the emission characteristics. Further study needs to be done into how the addition of nontypical gases to the CVD diamond process changes the structure of the films from that of cubic diamond. Control of the disorder of the film in this manner may make it possible to construct devices for electronic applications.

The authors would like to thank Max N. Yoder for providing the initiative to study the topic of cold cathodes and ballistic electron transport in thin-film materials. The authors are indebted to Professor P. H. Cutler, Dr. N. M. Miskovsky, and Dr. P. B. Lerner for stimulating discussions during this work. The authors are also thankful to Professor R. Messier for allowing them to use the vacuum system for the field-emission testing. This work was supported by the Office of Naval Research, with funding from the BMDO under Contract Nos. N00014-95-I905 and N00014-95-I-1051 and by the National Science Foundation under Grant No. DMR-95-22566.

- ¹C. A. Spindt, I. Brodie, L. Humphreys, and E. R. Westerberg, *J. Appl. Phys.* **47**, 5248 (1976).
- ²P. H. Cutler, Jun He, N. M. Miskovsky, T. E. Sullivan, and B. Weiss, *J. Vac. Sci. Technol. B* **11**, 387 (1993).
- ³A. G. Chynoweth, *Prog. Semicond.* **4**, 97 (1959).
- ⁴C. A. Mead, *J. Appl. Phys.* **32**, 648 (1961).
- ⁵S. D. Brorson, D. J. DiMaria, M. V. Fischetti, F. L. Pesavento, P. M. Solomon, and D. W. Dong, *J. Appl. Phys.* **58**, 1302 (1985).
- ⁶D. J. DiMaria, M. V. Fischetti, M. Arienzo, and E. Tierney, *J. Appl. Phys.* **60**, 1719 (1986).
- ⁷H. J. Fitting and A. Von Czarnowski, *Phys. Status Solidi A* **93**, 385 (1986).
- ⁸D. J. DiMaria and D. W. Dong, *J. Appl. Phys.* **51**, 2722 (1980).
- ⁹H. J. Fitting, G. O. Müller, R. Mach, G. U. Reinsperger, Th. Hingst, and E. Schreiber, *Phys. Status Solidi A* **121**, 305 (1990).
- ¹⁰G. O. Müller, R. Mach, G. U. Reinsperger, E. Halden, and G. Schulz, *J. Cryst. Growth* **117**, 948 (1992).
- ¹¹H. J. Fitting, Th. Hingst, E. Schreiber, and E. Geib, *J. Vac. Sci. Technol. B* **14**, 2087 (1996).
- ¹²H. J. Fitting, J. Blyde, and J. Reinhardt, *Phys. Status Solidi A* **81**, 323 (1984).
- ¹³H. J. Fitting and A. Von Czarnowski, *J. Cryst. Growth* **101**, 876 (1990).
- ¹⁴P. H. Cutler, Z. H. Huang, N. M. Miskovsky, P. D. Ambrosio, and N. M. Chung, *J. Vac. Sci. Technol. B* **14**, 2020 (1996).
- ¹⁵F. J. Himpsel, J. A. Knapp, J. A. Van Vechten, and D. E. Eastman, *Phys. Rev. B* **20**, 624 (1979).
- ¹⁶B. B. Pate, *Surf. Sci.* **165**, 83 (1986).
- ¹⁷J. Van der Weide and R. J. Nemanich, *J. Vac. Sci. Technol. B* **10**, 1940 (1992).
- ¹⁸M. W. Geis, J. C. Twitchell, and T. M. Lyszczarz, *J. Vac. Sci. Technol. B* **14**, 2060 (1996).
- ¹⁹P. Lerner, P. H. Cutler, and N. M. Miskovsky, *J. Vac. Sci. Technol. B* **15**, 1997 (1997).
- ²⁰K. Okano, Satoshi Koizumi, S. Ravi, P. Silva, and Gehan A. J. Amarantunga, *Nature (London)* **381**, 140 (1996).
- ²¹S. Jou, H. J. Doerr, and R. F. Bunshah, *Thin Solid Films* **280**, 256 (1996).
- ²²W. Zhu, G. P. Kochanski, S. Jin, and L. Seibles, *J. Vac. Sci. Technol. B* **14**, 2011 (1996).
- ²³A. Badzian and T. Badzian, *Int. J. Refract. Metals Hard Mater.* **15**, 3 (1997).
- ²⁴A. Badzian and T. Badzian, *Diam. Relat. Mater.* **2**, 147 (1993).
- ²⁵A. Badzian, T. Badzian, and S. Tong Lee, *Appl. Phys. Lett.* **62**, 3432 (1993).
- ²⁶P. H. Cutler, N. M. Miskovsky, and P. B. Lerner (private communication).